

# Passively $Q$ -switched laser with single longitudinal mode based on the frequency selection of grating and F-P etalon in twisted-mode folded cavity

Bao'an Song (宋宝安), Weijiang Zhao (赵卫疆), Deming Ren (任德明)\*, Yanchen Qu (曲彦臣), Heyong Zhang (张合勇), Liming Qian (钱黎明), and Xiaoyong Hu (胡孝勇)

National Key Laboratory of Tunable Laser Technology, Harbin Institute of Technology,  
Harbin 150001, China

\*E-mail: laser11@hit.edu.cn

Received November 30, 2008

A passively  $Q$ -switched side-pumped laser with folded resonator is specially constructed for single-longitudinal-mode smooth pulse output. Nd:YAG is chosen as the laser active medium and  $\text{Cr}^{4+}$ :YAG as the saturable absorber medium. Additionally, the method of frequency selection by grating with 1200 line/mm and Fabry-Perot (F-P) etalon is used in the twisted-mode cavity. The single-frequency smooth pulses are produced with 10-Hz repetition rate, 20-ns pulse width, and 1.064- $\mu\text{m}$  wavelength. The probability of single-frequency laser output measured is over 99% by using the methods of Fourier analysis and F-P etalon multiple-beam interferometry at the threshold voltage. The measured near-field and far-field angles of divergence are 1.442 and 1.315 mrad, respectively. The values of  $M^2$  are 1.32 and 1.31 separately with the knife-edge method. Single pulse at 1.064  $\mu\text{m}$  with the energy of 8.8 mJ is achieved in TEM<sub>00</sub> mode.

OCIS codes: 140.0140, 300.0300.

doi: 10.3788/COL20090709.0805.

Single-longitudinal-mode smooth pulse is widely attractive in a variety of applications such as the interferometer technique, optical communications, optical spectroscopy with high resolution, and Doppler wind lidar<sup>[1-3]</sup>. With the rapid development of Nd:YAG laser, side-pumped  $Q$ -switched or gain-switched Nd:YAG lasers become more and more important in these fields. Gain-switched Nd:YAG microchip lasers have produced single-frequency pulses with a repetition rate of 1 MHz and pulse width of 32 ns. Single-frequency operation is realized by temperature-tuning of the laser wavelength to the peak of the gain profile<sup>[4]</sup>. Besides, high repetition rate and compact laser sources can be realized by passive or active  $Q$ -switching (electro-optical or acousto-optical) of a laser diode (LD) or flash lamp pumped solid-state laser. But high repetition rate impacts the peak power and probability of single-frequency laser output with its poor thermal characteristic limits.

In order to achieve stable single-frequency laser output, the methods of three-plane resonant reflector<sup>[5]</sup>, twisted-mode cavity<sup>[6,7]</sup>, short-cavity<sup>[8]</sup>, seed injection, and frequency selection using Fabry-Perot (F-P) etalon and grating are usually used in Nd:YAG lasers. The length of cavity will be 1.5 cm if we use the method of short cavity. It is too short to meet actual energy requirement. The threshold is too high if the three-plane resonant reflector is used. The technique of seed injection is very complicated and the cost is high. The twisted-mode folded cavity is very suitable for adjusting light path to achieve stable single-frequency laser pulses with high probability of single longitudinal mode.

In this letter we investigate the optimization of single-frequency pulse laser. A side-pumped passively  $Q$ -switched laser with frequency selection of grating and

F-P etalon is put forward to solve the frequency jitter and shift in folded cavity. Though the repetition rate is not high, the probability of single-frequency pulse laser measured is over 99% using the methods of Fourier analysis and F-P etalon multiple-beam interferometry. The single-frequency operation takes place in the low pump power regime and different frequencies appear with the increase of pump power. Additionally, the values of  $M^2$  and divergence angle are measured using the beam propagation analyzer M<sup>2</sup>-101 and laser beam analyzer LBA-100A (both from SPIRICON).

For frequency selection, the circularly polarized light passes through the operation material in the twisted-mode cavity. The effect of spatial hole burning is eliminated and multimode oscillation is suppressed by the cavity. The problem of frequency jitter is settled with frequency selection of grating and F-P etalon. The principle is shown in Fig. 1. As shown in Fig. 1(a), multi-oscillation mode interval  $\Delta\nu_q$  is determined by the cavity length. The fluorescence linewidth of Nd:YAG is about 200 GHz. The linewidth  $\Delta\nu$  compressed by grating is about 20 GHz, as shown in Fig. 1(b). The narrowed linewidth is suitable for single-frequency pulse laser outgoing. Figure 1(c) shows the output longitudinal mode with fluorescence linewidth compressed by grating, in which there are three longitudinal mode outputs. Figure 1(d) is the transmission spectrum of F-P etalon with about 5-mm thickness and 80% index of reflection, where  $\Delta\text{FWHM}_2$  indicates the full-width at half-maximum of F-P etalon,  $\Delta\nu_{\text{FSR}_2}$  indicates the free spectrum range of F-P etalon. The stable single longitudinal mode is achieved by this method, as shown in Fig. 1(e).

The experimental setup is shown in Fig. 2. Nd:YAG was chosen as the laser active medium and  $\text{Cr}^{4+}$ :YAG as

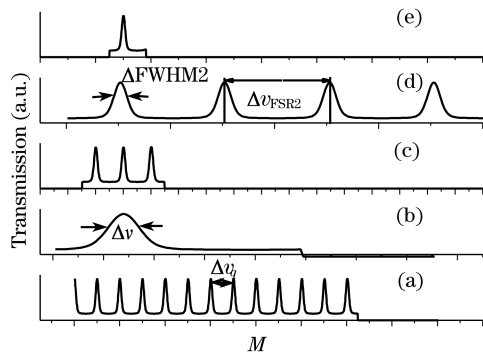


Fig. 1. Sketch about frequency selection of grating and F-P etalon. (a) Multi-oscillation mode; (b) fluorescence linewidth compressed by grating; (c) longitudinal mode outgoing with fluorescence linewidth compressed by grating; (d) transmission spectrum of F-P etalon; (e) final single longitudinal mode outgoing.  $M$  is the interference order.

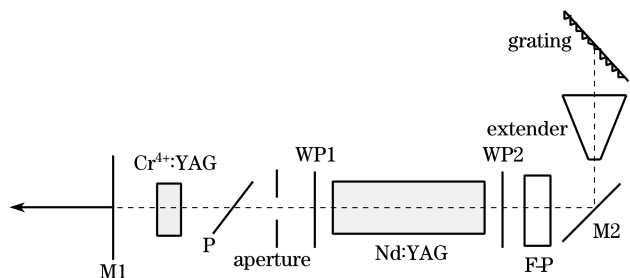


Fig. 2. Experimental setup for Nd:YAG laser based on twisted-mode folded cavity with frequency selection by grating and F-P etalon. WP1, WP2: 1/4 wave plates; M1, M2: mirrors; P: polarizer.

the saturable absorber medium. The diameter of aperture was 1.5 mm. The F-P etalon was coated with a reflectivity of 80%. The Nd:YAG chip was 80 mm in length and 5 mm in diameter. The laser was side-pumped by a flash lamp. The output mirror was coated for 30% reflectivity at 1.064  $\mu\text{m}$ . The mirror M2 was coated for a reflectivity of 99.9% at 45° and 1.064  $\mu\text{m}$ . The end surfaces of passively  $Q$ -switched crystal, 1/4 wave plate, and Nd:YAG crystal were coated for reducing reflection at 1.064  $\mu\text{m}$ . The maximum magnification of the expander was 25. The high reflectivity end was a grating of 1200 line/mm with a blazing wavelength of 1.064  $\mu\text{m}$ . The grating technique and auto collimation principle were applied in the solid-state laser with the folded resonator. The angle correction of the grating was realized by tuning the M2 at 45°. Besides, the folded resonator was very suitable for adjusting the light path. Because the laser pulses of 1.064  $\mu\text{m}$  were invisible, we used a He-Ne laser as the collimating light outside M2. The coincidence setting of the laser pulses with a wavelength of 1.064  $\mu\text{m}$  and He-Ne laser was not difficult.

The incident angle on the grating is determined by the grating equation:

$$m\lambda = d(\sin \alpha \pm \sin \beta), \quad (1)$$

where  $m$  is the diffraction number,  $\lambda$  is the laser wavelength,  $d$  is the grating constant,  $\alpha$  is the incident angle, and  $\beta$  is the diffraction angle. The grating generally works at the state of auto collimation in the laser resonator. So  $\alpha = \beta = \varphi_L$  with  $\varphi_L$  being the auto collimation

angle, and Eq. (1) can be written as

$$m\lambda = 2d \sin \varphi_L. \quad (2)$$

Because  $m$  is 1,  $\lambda$  is 1.064  $\mu\text{m}$ , and  $d$  is 1/1200 mm,  $\varphi_L$  is calculated to be 39.8°. So the incident angle is 39.8°. Firstly, we adjusted the outgoing mirror, high reflection mirror with 45° angle, and grating. The included angle between the normal line of grating and the optical axis was set at 39.8°. When the laser oscillation condition was about 330 V, this step was accomplished. Secondly, the 1/4 wave plates and polarizer were placed in the laser resonator. The separation angle between the optical axis of 1/4 wave plate and polarization direction was 45°. When the threshold voltage was about 350 V, we placed the passive  $Q$  switch and extender lens in the cavity. We must make light pass through the center of extender lens and the direction of propagation cannot be changed by it. When the threshold voltage was about 420 V, the extender lens was adjusted exactly. It was assembled in a four-dimensional (4D) laser optical bench. In the end, we placed the F-P etalon in the cavity. Through adjusting the F-P etalon, we can achieve smooth pulse output with single longitudinal mode at about 550-V threshold.

Figure 3 shows different pulse waveforms outgoing with different experimental conditions. Fourier spectra of these waveforms are separately shown in Fig. 4. From Fig. 4, we can see that there are four, three, two longitudinal modes, and a single longitudinal mode for Figs. 3(a)–(d), respectively. The laser multimode operation was not permitted in most interferometer techniques. We must reduce the probability of multimode operation. Through adjusting the angle of 1/4 wave plates and polarizer, the spatial hole burning phenomenon can be eliminated and smooth laser pulse output with single longitudinal mode can be achieved, as shown in Fig. 3(d) whose Fourier spectrum is shown in Fig. 4(d).

The laser longitudinal mode spacing is determined by the length of cavity. Before we measure the pulse waveforms, the mode spacing must be considered. The adjacent-pulse interval in the waveform is determined by the mode spacing. The response time of the detector and bandwidth of oscilloscope must meet the minimum pulse interval of waveform, otherwise, wrong results will

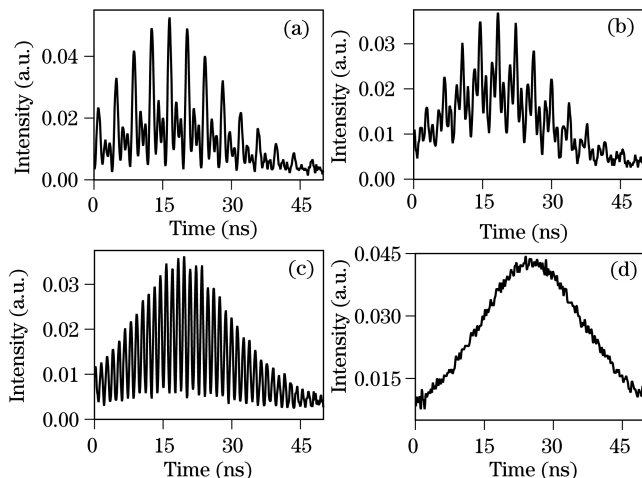


Fig. 3. Output laser pulse waveforms under different experimental conditions.

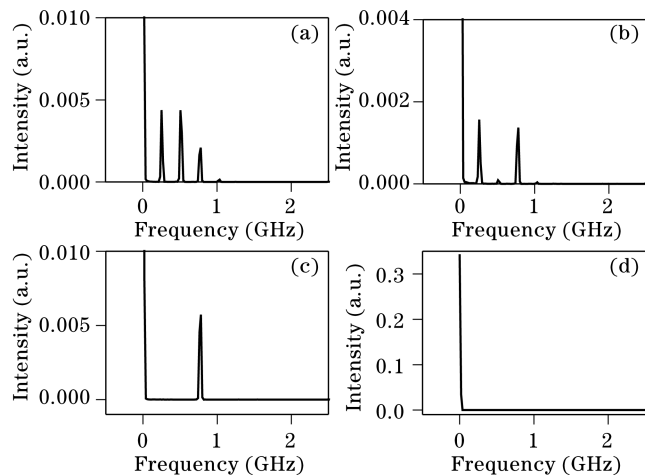


Fig. 4. Fourier spectra of pulse waveforms corresponding to Figs. 3(a)–(d). (a) Four longitudinal modes; (b) three longitudinal modes; (c) two longitudinal modes; (d) single longitudinal mode.

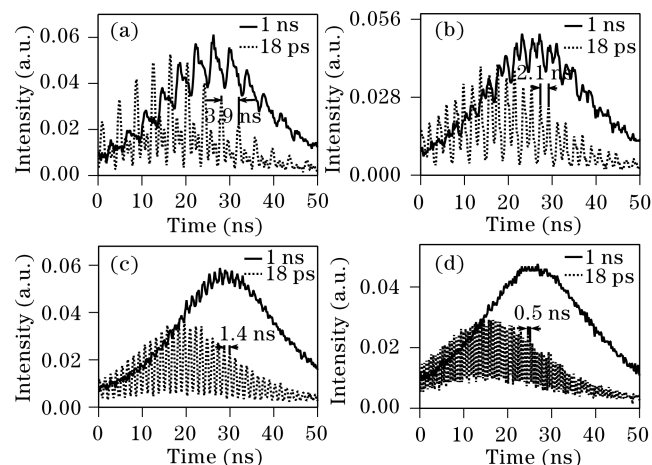


Fig. 5. Pulse waveforms measured with detectors of different response time. (a) Pulse interval is 3.9 ns; (b) pulse interval is 2.1 ns; (c) pulse interval is 1.4 ns; (d) pulse interval is 0.5 ns.

**Table 1. Parameters of F-P Etalon and CCD in Experiment**

Thickness of F-P (mm)	Reflectivity of F-P	Aperture of F-P (mm)
20	90%	30
Resolution of CCD	Pixel Size ( $\mu\text{m}$ )	Response Wavelength Range of CCD (nm)
576×768	12	400-1100

be yielded. As shown in Fig. 5, the solid lines are measurement results by the detector with a response time of 1 ns, while the dash lines are measurement results by the detector with a response time of 18 ps (NEW FOCUS). The oscilloscope was TDS7254B with 2.5-GHz bandwidth. We can see that the solid waveform is distorted when the pulse interval is less than 1 ns. In our experiment, the ultimate range multimode spacing was about 2 GHz, so the response time must be faster than 500 ps.

The phenomenon of frequency jitter and multimode

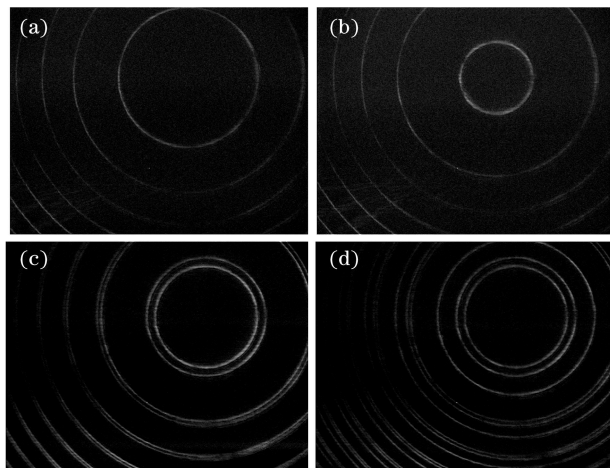


Fig. 6. Sharp interference fringes. (a) Single longitudinal mode case 1; (b) single longitudinal mode case 2; (c) two longitudinal modes; (d) three longitudinal modes.

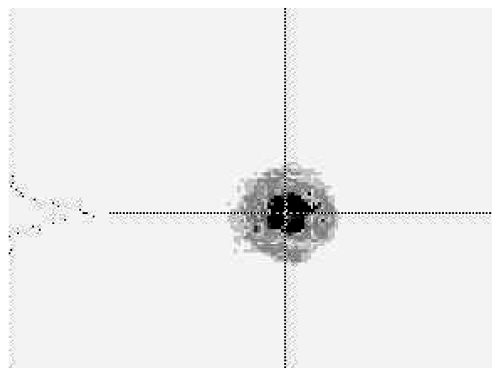


Fig. 7. Distribution of transverse mode.

was researched with the method of multiple-beam interferometry. The interference fringe was imaged on a plane charge-coupled device (CCD). The parameters of the plane CCD and F-P etalon are shown in Table 1. The measured sharp interference fringes are shown in Fig. 6. When the interference fringe is similar with Fig. 6(a) or (b), the laser works with single longitudinal mode. The different diameters of the center interference rings show that the laser works with different longitudinal modes. This is the phenomenon of frequency jitter. The pulse laser output with multimode operation is shown in Figs. 6(c) and (d), which separately show that the laser works with two and three longitudinal modes.

Through adjusting the angles of grating and F-P etalon, the frequency jitter can be suppressed. The probability of multimode operation can be reduced with careful alignment of the  $1/4$  wave plates to the polarizer. It was less than 1% when the laser was in good working order.

The transverse mode of laser was researched by the equipment of beam propagation analyzer M<sup>2</sup>-101 and laser beam analyzer LBA-100A. The measuring results are shown in Fig. 7. In this experiment the beam was directed into the equipment. The optical intensity was changed by using the tunable attenuation plate. The prism and reflecting mirror cannot be used in the light path to achieve accurate measuring results. The equip-

ment worked with the mode of screen triggering.

As shown in Fig. 7, the transverse mode was  $TEM_{00}$  with Gaussian distribution. The near-field and far-field angle of divergence were 1.442 and 1.315 mrad, respectively. The values of  $M^2$  were separately 1.32 and 1.31.

In conclusion, a side-pumped passively  $Q$ -switched laser with folded resonator and frequency selection of grating and F-P etalon is put forward to solve the frequency jitter and shift in the twisted-mode folded cavity. The probability of single-frequency pulse laser measured is over 99% by using Fourier analysis and F-P etalon multiple-beam interferometry. The detailed operation schedule is described. The results show that the frequency jitter and multimode operation are suppressed with a careful alignment. The threshold voltage is about 500 V. With the increase of working voltage, different frequencies appear. Additionally, the divergence angles and  $M^2$  values are measured. Single pulse at  $1.064 \mu\text{m}$  with energy of 8.8 mJ is achieved in a  $TEM_{00}$  mode.

## References

1. X. Sun, J. Liu, J. Zhou, and W. Chen, *Chin. Opt. Lett.* **6**, 679 (2008).
2. B. M. Gentry, H. Chen, and S. X. Li, *Opt. Lett.* **25**, 1231 (2000).
3. B. Song, W. Zhao, D. Ren, Y. Qu, Y. Bai, S. Mo, S. Zhang, and X. Hu, *Acta Opt. Sin.* (in Chinese) **28**, 787 (2008).
4. Y. Wang, L. Huang, M. Gong, H. Zhang, M. Lei, and F. He, *Laser Phys. Lett.* **4**, 580 (2007).
5. W. He and Z. Lü, *Chinese J. Lasers* (in Chinese) **28**, 1063 (2001).
6. Q. Liu, M. Lei, M. L. Gong, L. Huang, F. H. He, X. Fu, and X. P. Yan, *Appl. Phys. B* **89**, 155 (2007).
7. H. Pan, S. Xu, and H. Zeng, *Opt. Express* **13**, 2755 (2005).
8. Y. Ju, Z. Wang, L. Wang, and Y. Wang, *Acta Opt. Sin.* (in Chinese) **28**, 2164 (2008).